

Near-Field Optical Imaging and Spectroscopy of Single GaAs Quantum Wires

V. EMILIANI¹⁾ (a), F. INTONTI (a), CH. LINEAU (a), T. ELSAESSER (a), R. NÖTZEL (b), and K. H. PLOOG (b)

(a) *Max-Born-Institute für Nichtlinear Optic und Kurzzeitspektroskopie, Berlin, Germany*

(b) *Paul Drude Institute für Festkörperelektronik, 10117 Berlin, Germany*

(Received September 4, 2001; in revised form October 5, 2001; accepted October 12, 2001)

Subject classification: 78.55.Cr; 78.67.Hc; 78.67.Lt; S7.12

Low-dimensional semiconductor structures grown by molecular beam epitaxy on a patterned (311)A GaAs substrate are investigated by near-field spectroscopy at a temperature of 10 K. In particular, the two-dimensional potential profiles of quantum wire and coupled wire–dot structures are determined from photoluminescence (PL) measurements with a spatial resolution of 150 nm. Also presented is an optical method for investigating carrier transport in low-dimensional systems involving performing spatially resolved PL excitation measurements on the wire–dot structure.

Introduction In recent years the aim of research in low-dimensional physics has been to move beyond traditional ensemble studies to probe semiconductor nanostructures on sub-wavelength length scales, i.e. small enough to isolate the optical, topographical, or, more generally, the quantum mechanical signatures of single quantum wires (QWRs) or quantum dots.

In this paper we report on a near-field optical study of a GaAs/AlGaAs wire–dot structure grown by molecular beam epitaxy (MBE) on a patterned GaAs (311)A substrate. The combination of this growth technique with appropriate lithographic patterning of the substrate allows one to control the layer width variations on the growth surface to form a coupled QWR–dot structure [1]. The aim of our investigation was to study the carrier transport within these low-dimensional nanostructures by optical methods.

Experimental The GaAs/AlGaAs nanostructures were grown by MBE on patterned GaAs (311)A substrates. In such structures, QWRs are formed due to the preferential migration of Ga ad-atoms from the mesa top and bottom towards one of the sidewalls of mesa stripes oriented along [01–1]. In particular, a coupled QWR–dot structure was realized by growing a zigzag pattern with sidewalls alternately misaligned by $\pm 30^\circ$ from [01–1] [1]. The samples consisted of a GaAs quantum well (QW) layer clad between 50 nm Al_{0.5}Ga_{0.5}As barriers, covered with a 20 nm GaAs protective layer. Two samples (A and B) were investigated: one (sample A) with a QW thickness of 6 nm and straight QWRs; the GaAs QW of the second (sample B) was 3 nm thick and had a zigzag patterning (Fig. 1a, a schematic top view).

Two-dimensional (2D) near-field images were obtained at variable temperatures (T) with a home-built near-field optical microscope [2]. For the high-energy-resolution

¹⁾ Corresponding author; Phone: 39 055 2307832; Fax: 39 055 224072;
e-mail: emiliani@lens.unifi.it

images, the microscope was used in the illumination/collection geometry. The excitation laser beam (photon energy of 1.96 eV) was transmitted through the fibre tip and the photoluminescence (PL) emitted from the sample was collected through the same fibre. PL spectra were acquired with an $f = 50$ cm monochromator in conjunction with a liquid nitrogen-cooled CCD camera. For the optical transport measurements, the microscope was used in the illumination geometry. A tunable Ti:sapphire laser was coupled into the fibre tip for the excitation. The PL emission was collected in far field through a conventional microscope objective and detected with a silicon avalanche photodiode. Near-field probes were made by chemically etching single-mode optical fibres. In the illumination mode they were coated with a 100 nm thick aluminium layer.

Results and Discussion The inset of Fig. 1b shows a far-field spectrum of sample B. Three major emission peaks at 1.64, 1.67, and 1.72 eV and a weak shoulder at 1.74 eV are visible. Their spatial origin is revealed by 2D near-field images shown in Figs. 1b–e. The emission at the lowest energy (1.64 eV) originates from the corners of the two intersecting sidewalls that point toward the mesa top. At these positions dot-like regions are formed. For detection at 1.67 eV we find the QWR emission, interrupted around the position where the first image reveals dot formation. The PL at 1.72 eV extends on both mesa top and bottom and originates from exciton recombination in the flat QW area. Figure 1e shows the spatial distribution of the PL signal at 1.74 eV (the weak shoulder). The photon energy from this region is higher than both the QW and the QWR emissions, i.e. represents an energy *barrier* between the mesa top and the QWR [3, 4]. The existence of an energy barrier at the wire–well interface is also revealed by the PL images from sample A (Fig. 2). Figure 2a shows the location of the QWR, while Figs. 2b–d show the emission from the QW: a blue shift in the emission is evident from the mesa top with respect to the mesa bottom. Figures 2e and f show the emission from the barriers that in this sample are visible on both sides of the wire.

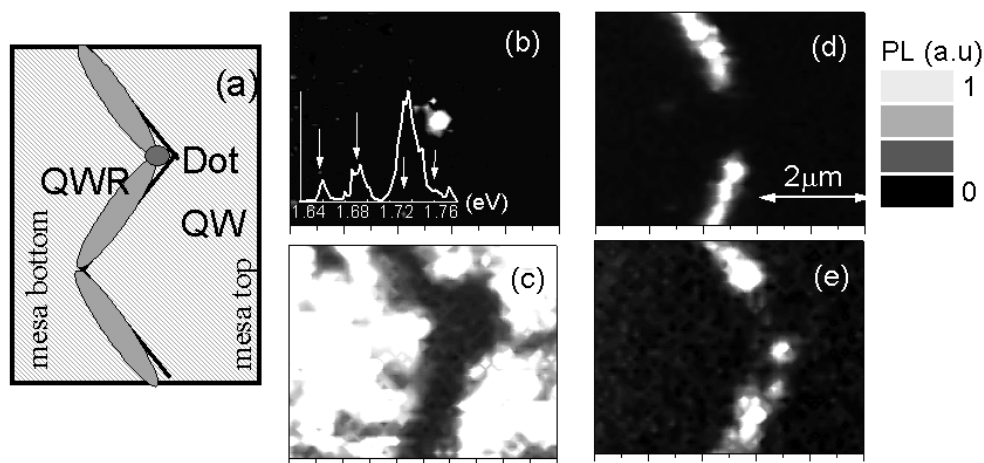


Fig. 1. a) Schematic of the structure of sample B. Two-dimensional PL images of sample B at 10 K taken at different detection energies: b) 1.642 eV; c) 1.674 eV; d) 1.721 eV; e) 1.745 eV. The detection energies are indicated with arrows in the inset, which shows the far-field PL spectrum

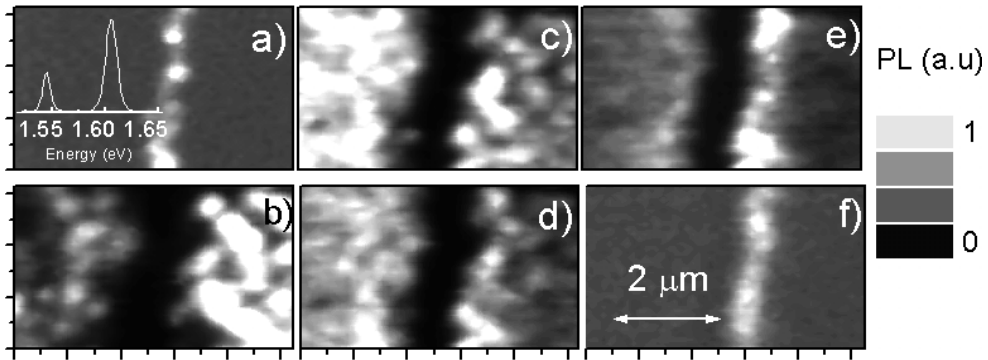


Fig. 2. Two-dimensional high-energy-resolution images from sample A taken at 10 K and at different detection energies: a) 1.544 eV; b) 1.597 eV; c) 1.605 eV; d) 1.610 eV; e) 1.614 eV; f) 1.627 eV. The inset shows the far-field spectrum

As already discussed in Ref. [4], the change in the local emission energy originates mainly from a change in the local thickness of the GaAs layer. From the PL images one can derive a 2D map of the average exciton emission energy and then evaluate the variation of the local GaAs layer thickness. The average emission energy is extracted by summing, at each position of the tip, all the emission energies weighted by the corresponding emission intensity. A 2D map of the GaAs layer thickness can be finally calculated by solving the reverse problem of a finite well in the effective-mass approximation [5]. The results of this calculation show an energy barrier of up to 20 meV on the top mesa side of sample B, corresponding to a local decrease of the average thickness down to 2.9 nm (1 monolayer (ML)) in respect to the flat QW. Barrier heights of up to 40 meV have been measured for sample A, corresponding to a local decrease of the GaAs QW thickness of up to 4 ML. The thinning of the QW in the proximity of the sidewall is a consequence of Ga ad-atom migration towards the sidewall during the growth process. This migration gives rise to the formation of a thicker GaAs region at the edge (QWR formation) surrounded by thinner regions in the adjacent parts at the top and bottom areas. The asymmetry of the potential barriers reflects a strong asymmetry of the diffusion coefficient in the mesa top and bottom. This result is confirmed by modelling the formation of the surface patterns during growth using a simplified analytical model [5].

Contrary to what has been observed at the well-wire interface, no energy barriers were detected at the dot-wire boundary [5]. This topological property is crucial for the transport experiment described in what follows. We measured the diffusion coefficient in the coupled dot-wire structure by recording near-field PL excitation (PLE) images of the dot area. The detection energy was fixed at the dot emission (1.64 eV) and the excitation energy was varied. Images of the dot emission were taken at three excitation energies, $E_{\text{ex}}(\text{QW})$, $E_{\text{ex}}(\text{QWR})$, and $E_{\text{ex}}(\text{Dot})$, selected to create carriers resonantly with the lowest QW, QWR, and dot transitions. At 80 K (Fig. 3) the PL spatial distribution is strongly modified, depending on the excitation energy. It has a circular shape in the case of the QW excitation and shows broad tails that extend exponentially into the wire region in the case of QWR excitation. Finally, for resonant dot excitation we find

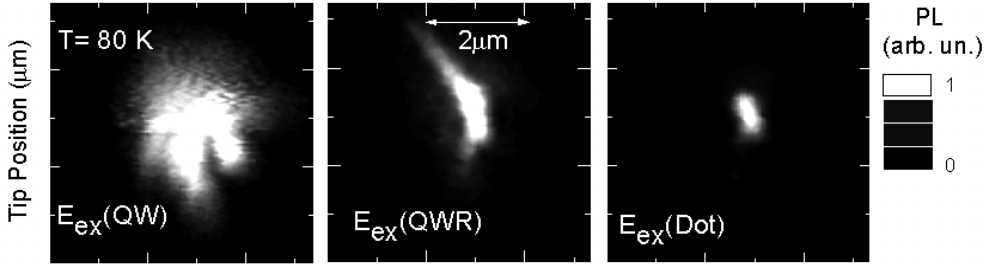


Fig. 3. Two-dimensional near-field PLE images recorded at 80 K. The excitation energies $E_{\text{ex}}(\text{QW})$, $E_{\text{ex}}(\text{QWR})$, and $E_{\text{ex}}(\text{Dot})$ are selected in order to create carriers resonantly with QW, QWR, and dot transitions. The detection energy is tuned at the dot PL peak

the dot image convoluted with the spatial resolution. In a steady-state diffusion model, the PL signal $I_{\text{dot}}(x)$ is expected to decrease exponentially with increasing distance from the dot: $I_{\text{dot}}(x) \propto \exp(-|X|/L)$, where L is the diffusion length and X the distance between the tip and the dot.

From Fig. 3 it is possible to extract the PL intensity profile when the tip is moved within the embedding QW and along the QWR axis and to deduce the 2D and 1D diffusion length. Values of $L_{\text{QW}} = 650 \pm 100$ nm and $L_{\text{QWR}} = 600 \pm 100$ nm are derived for the QW and QWR diffusion length, respectively.

From the low- T data, where the spatial profile of the dot PL is limited by the spatial resolution, we extract for the diffusion lengths L_{QW} and L_{QWR} an upper limit of 120 nm. From the observed diffusion lengths and the measured [4] lifetimes $\tau_{\text{QW}} = 1.3$ ns and $\tau_{\text{QWR}} = 1.5$ ns, one can estimate the 2D and 1D diffusion coefficients $D_{\text{QW}} = L_{\text{QW}}^2/\tau_{\text{QW}}$, and $D_{\text{QWR}} = L_{\text{QWR}}^2/2\tau_{\text{QWR}}$, and the corresponding mobilities μ_{QW} and μ_{QWR} . From the data shown in Table 1 and previously reported results [6, 7], two main aspects are evident: first, the similarity between the 2D and the 1D diffusion coefficients; and second, the strong dependence, in both cases, on T . We conclude that in both cases the mobilities are dominated by interface scattering. At the lowest temperatures, the rapid relaxation of optically excited electron-hole pairs into localized exciton states reduces the diffusion length to less than the resolution of our experiment. At elevated T , scattering with acoustic phonons induces exciton escape out of their local potential minima and enhances the mobility. At least in nanostructures with finite disorder, the resulting exciton mobilities appear to be less sensitive to the dimensionality of the nanostructure than to the details of the disorder potential [8].

Table 1

Exciton diffusion coefficients and mobilities obtained from the profiles of the images in Fig. 3

T (K)	D_{QW} (cm ² /s)	D_{QWR} (cm ² /s)	μ_{QW} (cm ² /Vs)	μ_{QWR} (cm ² /Vs)
10	≤ 0.1	≤ 0.05	≤ 115	≤ 60
80	3	1.2	435	174

Conclusions We have presented low-temperature near-field spectroscopic experiments on single AlGaAs/GaAs QWRs. An analysis of the high spatial resolution PL images gives potential energy profiles of the structures. A potential barrier originating from local thinning of the GaAs layer at the well–wire interface has been detected in both structures. The wire–dot structure was used to investigate optically carrier transport in single QWRs: the dot was exploited as an optical marker for exciton diffusion via QW and QWR states. The measured values for the diffusion coefficient and their dependence on the temperature suggest that in both the QW and QWR regions scattering by interface roughness dominates the transport properties.

Acknowledgements This work was supported by the Deutsche Forschungsgemeinschaft (SFB296) and by the European Union through the EFRE programme. V.E. gratefully acknowledge the TMR programme for financial support under the proposal ERB4001GT975127.

References

- [1] J. FRICKE et al., J. Appl. Phys. **85**, 3576 (1999), and references therein.
- [2] G. BEHME, A. RICHTER, M. SÜPTITZ, and CH. LIENAU, Rev. Sci. Instrum. **68**, 3458 (1997).
- [3] A. RICHTER et al., Appl. Phys. Lett. **73**, 2176 (1998).
- [4] CH. LIENAU et al., Phys. Rev. B **58**, 2045 (1998).
- [5] V. EMILIANI et al., Phys. Rev. B **64**, 155316 (2001).
- [6] H. HILLMER et al., Phys. Rev. B **39**, 10901 (1989).
- [7] H. HILLMER, A. FORCHEL, R. SAUER, and C. W. TU, Phys. Rev. B **42**, 3220 (1990).
- [8] F. INTONTI et al., Phys. Rev. Lett. **87**, 076801 (2001).

